Chaos
An Interdisciplinary Journal of Nonlinear Science

RESEARCH ARTICLE | SEPTEMBER 19 2024

Investigation of transient extreme events in a mutually coupled star network of theoretical Brusselator system FREE

S. V. Manivelan ; S. Sabarathinam ; K. Thamilmaran; I. Manimehan

Chaos 34, 091102 (2024)
https://doi.org/10.1063/5.0232021

Investigation of transient extreme events in a mutually coupled star network of theoretical Brusselator system

Cite as: Chaos 34, 091102 (2024); doi: 10.1063/5.0232021
Submitted: 4 August 2024 · Accepted: 2 September 2024 ·
Published Online: 19 September 2024

S. V. Manivelan,[1] S. Sabarathinam,[2] K. Thamilmaran,[3] and I. Manimehan[1,a)]

AFFILIATIONS

[1]Department of Physics, M. R. Government Arts College (Affiliated to Bharathidasan University, Tiruchirappalli), Mannargudi 614 001, Tamilnadu, India
[2]Laboratory of Complex Systems Modeling and Control, Faculty of Computer Science, National Research University, Higher School of Economics (HSE), Moscow 109028, Russia
[3]Centre for Computational Modeling, Chennai Institute of Technology, Chennai 600 069, Tamilnadu, India

[a)]**Author to whom correspondence should be addressed:** manimehan@gmail.com

ABSTRACT

In this article, we present evidence of a distinct class of extreme events that occur during the transient chaotic state within network modeling using the Brusselator with a mutually coupled star network. We analyze the phenomenon of transient extreme events in the network by focusing on the lifetimes of chaotic states. These events are identified through the finite-time Lyapunov exponent and quantified using threshold and statistical methods, including the probability distribution function (PDF), generalized extreme value (GEV) distribution, and return period plots. We also evaluate the transitions of these extreme events by examining the average synchronization error and the system's energy function. Our findings, validated across networks of various sizes, demonstrate consistent patterns and behaviors, contributing to a deeper understanding of transient extreme events in complex networks.

The phenomenon of transient chaos has been extensively researched across diverse domains, including hydrodynamics, ecology, economics, coupled electronic circuits, electrophysiology, neural networks, and power grids. Additionally, the occurrence of extreme events (EEs) in these fields has demonstrated profound impacts, leading to a crucial question: Do extreme events emerge during a transient chaotic state in complex networks? This underscores the importance of investigating the EE phenomenon within transient chaotic systems. However, the precise identification and characterization of transient extreme events (TEEs) have not been addressed in the existing literature. In this article, we identify extreme events that emerge during the transient state from both a dynamical system and network perspective. This study provides the first evidence of transient extreme events within network and mathematical modeling, offering valuable insights into real-world occurrences. Here, we investigate the emergence of typical extreme events and transient extreme events within a mutually coupled star network of the Brusselator model. The identification of TEEs was accomplished using the finite-time Lyapunov exponent and statistical methods, which are employed to assess rare events. Additionally, we investigated the transitions of EEs by evaluating the average synchronization error and the system's energy, which quantifies the degree of coherence among the oscillators in the network. To validate the robustness and generalizability of our results, we expanded our study to networks of varying sizes, consistently identifying similar patterns and phenomena. This detailed analysis not only deepens our comprehension of TEEs but also opens up possible potential applications across various scientific and engineering fields, including enhancing the reliability of mathematical models and forecasting extreme events.

I. INTRODUCTION

In recent years, there has been a noticeable increase in attention toward investigating extreme events, which are occurrences in dynamical systems that happen suddenly and exhibit unusual

dynamical phenomena. Extreme events phenomena are extensively studied within various isolated dynamical systems,[1,2] providing critical insights into their underlying mechanisms. However, real-world scenarios often involve dynamical systems that are not isolated but are components of larger, interconnected networks. Studying extreme events in the context of networks is crucial for understanding the occurrence and impact of extreme events in both natural systems, such as ecological networks,[3] neuron networks,[4] and man-made systems.[5,6] Hence, the extreme events phenomenon is observed across various types of network models, including static networks,[7] random walks on networks,[8,9] scale-free networks,[10] multilayer, interdependent complex networks,[11] and time-varying networks.[12]

Therefore, a wide range of natural and man-made phenomena are studied in scale-free topology,[13,14] and the star network motif, representing scale-free networks, consists of a central hub node connected to several peripheral nodes, and star network makes it an ideal model for understanding the dynamics of scale-free networks. Furthermore, numerous intriguing dynamical behaviors such as chimera states,[15] remote synchronization,[16] and explosive synchronization[17] have been demonstrated regarding the star network motifs in phase oscillators,[16] the spread of an epidemic[18] and this network found within neural networks[19] that play vital roles in both cognitive processes[20] and sensory functions.[21] However, the phenomenon of extreme events has not yet been studied in this network.

Moreover, prior research has shown that extreme events emerge within chaotic and nonchaotic systems[22] in isolated, coupled, or networked dynamical systems. The interesting question arises: is the behavior of the extreme events induced during the transient state, and if so, how does it manifest in the asymptotic state? In the past, transient chaos has been extensively studied in various fields, such as hydrodynamics,[23] ecology,[24] economics,[25] coupled electronic circuits,[26] electrophysiology,[27] neural networks,[28] and power grids.[29] Similarly, significant impacts of extreme events[30] have been observed in these same fields. However, while these phenomena have been explored independently, this underscores the importance of investigating the EE phenomenon within transient chaotic systems. Additionally, transient chaos exhibits over very long iterations of the transient period[31,32] and extreme transient behaviors, where the system's transient states become extremely prolonged and occur spontaneously.[33] This makes it particularly interesting to investigate the behavior of extreme events in the transient state of a system, which is responsible for the system's asymptotic state. Hence, we classified the extreme events in the system's transient state as a special class of extreme events, which we denote as transient extreme events (TEEs).

Besides, the first experimental demonstrations of chaotic behavior in chemical oscillators were observed in the Belousov–Zhabotinsky (BZ) reaction.[34] Since then, the BZ reaction has been extensively studied in isolated, coupled, and network systems, showcasing a wide range of nonlinear phenomena, including Turing patterns, waves, clusters, and chaos.[35,36] However, investigations into BZ reactions in star network configurations remain limited, and experimental studies in these networks[37] have created significant interest in star network configurations. In the context of chemical oscillators, we recently investigated extreme events in the Brusselator model[38] influenced by an external periodic force for the first time. Motivated by the previous research on star network configurations of the Belousov–Zhabotinsky reaction, this article explores extreme events and transient extreme events (TEEs) using the theoretical Brusselator model in a star network configuration.

This article is organized as follows: Sec. II describes the mathematical model. Section III provides the numerical analysis, covering transient lifetime , generalized extreme value distribution, average synchronization error, and the system's energy function. Section IV discusses the significance and potential applications of this study. Finally, Sec. V presents the conclusions.

II. MODEL DESCRIPTION

We consider a coupled Brusselator oscillator arranged in a star network topology as defined by the $N \times N$ connectivity matrix A_{nm},

$$A_{nm} = \begin{cases} 1 & \text{if } n = 1 \text{ or } m = 1 \text{ and } (n,m) \neq (1,1), \\ 0 & \text{otherwise,} \end{cases}$$

and where each oscillator ($n = 2, \ldots, N$) in the network is coupled to the central hub oscillator ($n = 1$) as displayed in Fig. 1 through the cross-feedback, which is symmetric owing to bidirectional couplings. The governing equations are provided by

$$\begin{aligned} \dot{x_n} &= a - bx_n - x_n + x_n^2 y_n, \\ \dot{y_n} &= bx_n - x_n^2 y_n + \frac{\varepsilon}{d_n} \sum_{m=1}^{N} A_{nm}(x_m - x_n), \end{aligned} \tag{1}$$

where $n = 1, 2, \ldots, N$. The system state variables are x and y, which represent concentrations of autocatalysts, while a and b are constant system parameters representing concentrations of reactants and ε represents the global chemical coupling strength. $d_n = (N - 1, \underbrace{1, 1, \ldots, 1}_{N-1 \text{ times}})$ represents the in-degree of node n, which is used for normalizing the input toward nodes. The equilibrium points for the system equation (1) are obtained by setting the derivatives of x and y with respect to time equal to zero. Thus, the system has only one equilibrium point in each oscillator, which is $(x_{n_0}, y_{n_0}) = (a, b/a)$. The characteristic eigenvalue equations derived for the equilibrium point of an N oscillator are

$$\lambda_{1,\ldots,2N} = \frac{-(a^2 - b + 1) \pm \sqrt{(a^2 - b + 1)^2 - 4a^2(\alpha\,\varepsilon + 1)}}{2},$$

$$\text{where} \begin{cases} \lambda_{1,2} & \text{for } \alpha = 0, \\ \lambda_{3,4} & \text{for } \alpha = 2, \\ \lambda_{5,\ldots,2N} & \text{for } \alpha = 1. \end{cases}$$

Hence, the equilibrium points stability depends on the system parameters of a and b. If $b > (a^2 + 1)$, the equilibrium point is *unstable*. If $b < (a^2 + 1)$, it is *stable*. When $b = (a^2 + 1)$, it can be a *center* or an *ellipticpoint*, showing oscillatory behavior.

III. NUMERICAL RESULTS

Our study of the proposed network system (1) began with an analysis of its dynamics using a bifurcation diagram and

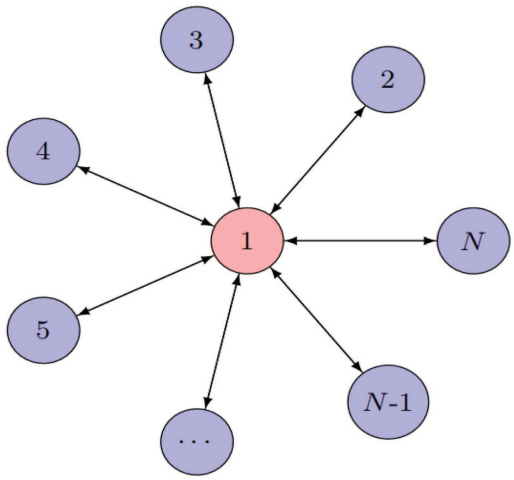

FIG. 1. Schematic view of a star network composed of N nodes. The central hub is $n = 1$ in a red solid circle and the peripheral nodes are $n = 2, \ldots, N$ in blue solid circles.

its corresponding Lyapunov spectrum of the central hub with varying coupling strength (ε) within the range of $\varepsilon \in (0, 1)$. Here, for convenience in the present study, we contemplate a system consisting of a total of $N = 6$ nodes for an oscillatory network, with other system parameters being constant as $a = 0.21$ and $b = 1.061$. For all numerical analyses, the initial conditions for the oscillators in the network were set as $(x_i(0), y_i(0)) = (0.01, 0.01)$ if i is odd, $(0.02, 0.02)$ if i is even. The system demonstrates distinct complex dynamics under varying initial conditions, which will be discussed in Sec. III B. A bifurcation diagram is computed for the transient and asymptotic states with a step size of 0.01. The transient state is depicted in Fig. 2(a) in blue color dots, calculated for the iterations of $T = 2 \times 10^4$–2×10^5 time units. The asymptotic state is depicted in Fig. 2(a) in red color dots, calculated for the iterations of $T = 2 \times 10^5$–7×10^5 time units. Our analysis revealed that the network demonstrates periodic behavior in both transient and asymptotic states at weak coupling.

However, at coupling strength $\varepsilon = 0.16$, a sudden expansion occurs in the amplitude of the network, resulting in an extreme events within both system states. This phenomenon persists until the coupling strength reaches $\varepsilon = 0.605$ in the asymptotic state, at this point, the system returns to a periodic state due to synchronization across the network induced by strong coupling. This transition from a chaotic state to a completely synchronized state takes a prolonged time to settle, inducing transient chaos with extreme events embedded within systems. The system exhibits extreme events only in the transient state; this events region is depicted as a rectangular box in Fig. 2(a) from $\varepsilon = 0.483$ to 0.605. We named this new phenomenon as transient extreme events (TEEs), which is the system that exhibits the extreme events occurrence within a transient chaotic state. Section III A explains this new phenomenon using relevant numerical and statistical measures.

To examine the typical extreme events behavior in our network, the numerically obtained time series is depicted in Fig. 3.

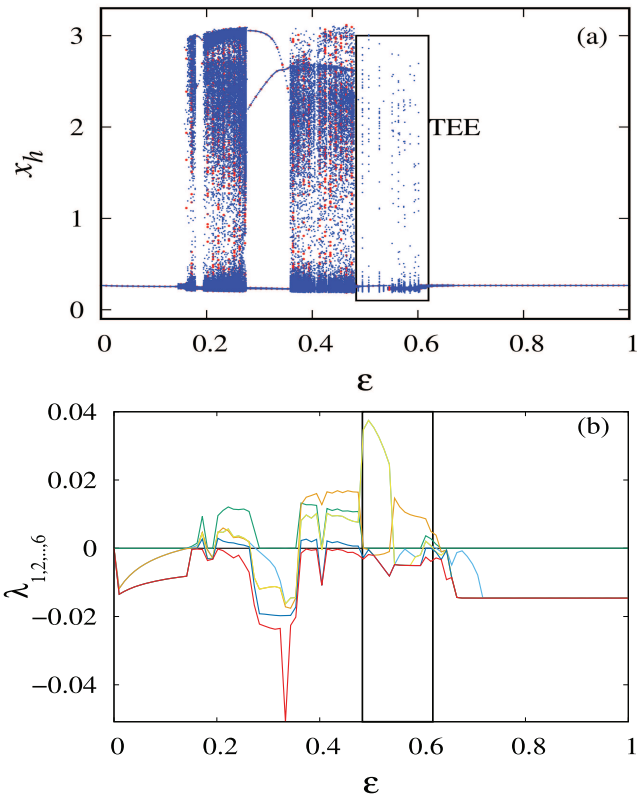

FIG. 2. The panel shows (a) the bifurcation diagram of the central hub x_h, with the transient state depicted as blue dots and the asymptotic state as red dots. (b) displays the Lyapunov exponent of the system central hub.

Throughout the entire iteration, the system parameters are fixed as given above, and the global coupling strength is set to $\varepsilon = 0.1657$; hence, the system shows chaotic behavior, and its trajectory spontaneously exhibits extreme events (rare events). To distinguish extreme events from normal events, a threshold height (H_s) is determined using a statistical approach that identifies significant deviations from the mean value of the system's state variable. Here, H_s is calculated as $H_s = \langle x_{\max} \rangle + m\sigma_{x_{\max}}$, where $\langle x_{\max} \rangle$ represents the mean of the peak state variable, $\sigma_{x_{\max}}$ is the standard deviation of $x_{\max}$, and m is an integer specific to the system. To validate the existence of EEs, we plotted the critical threshold ($H_s = 1.3152$) in the time series ($x_h(t)$) as a dashed horizontal line for $m = 8$, as illustrated in Fig. 3(a). This abrupt expansion of the network is classified as an extreme events. To confirm that the system is in an asymptotic state,[39] very long-time iterations of $T = 1 \times 10^8$ were taken to allow the system to evolve. To confirm the presence of extreme events in the proposed model, we have plotted the probability distribution function for the state variable $x_h(t)$ of the central hub. We considered a long time span, running the system for 2×10^8 time units and allowing it to evolve through transient states with constant parameters as used previously.

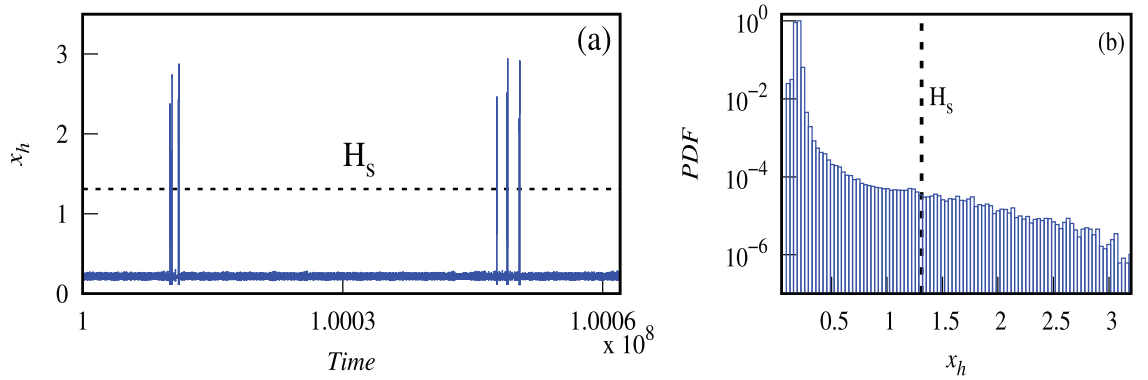

FIG. 3. Numerically computed (a) time evolution of typical extreme events of the state variable $x_h(t)$ with the threshold ($H_s = 1.3152$) marked as a horizontal dashed line for $m = 8$, and (b) the corresponding probability distribution function (PDF) with the threshold marked as a vertical dashed line.

Figure 3(b) shows a continuously heavy-tailed distribution, surpassing the threshold indicated by the vertical dotted black line. This indicates the occurrence of extreme events and confirms the low probability of large-amplitude events occurring beyond the H_s mark, which is calculated for $m = 8$ using the respective probability distribution function data of $\varepsilon = 0.1657$ to confirm the presence of the typical extreme events in the network.

A. Transient extreme events

To study the phenomenon of transient extreme events in the proposed network Eq. (1), we present our primary findings from the numerically obtained time series of the central hub ($x_h(t)$), as shown in Fig. 4. For the global coupling strength $\varepsilon = 0.6$, the system exhibits transient chaos, displaying chaotic behavior for long-time iterations of 1.4388×10^5 before settling into a periodic state. This transient chaotic state exhibits extreme events in every oscillator of the network and these events are characterized by threshold height (H_s). We observed that chaotic state behavior remains confined to the transient state, with the EE behavior showing a sudden expansion in phase space, represented in blue color in Fig. 4(a). In the asymptotic state, the system settles into a periodic state, represented in red color as shown in the subplot of Fig. 4(a). This transient chaotic behavior is confined to a specific temporal region, with the EE phenomenon characterized by rare and extreme amplitude bursts, depicted in blue color in Fig. 4(b). After a transient state, the system settles into a periodic state (period 10 limit cycle), represented in Fig. 4(b) with a red color. For the case of transient extreme events with $\varepsilon = 0.6$, the probability distribution function is depicted in Fig. 4(c), which shows a continuously heavy-tailed distribution that exceeds the threshold value indicated by the vertical dotted black line. This demonstrates the occurrence of extreme events during the transient state, depicted in blue color, beyond the H_s threshold, confirming the low probability of large-amplitude events. Additionally, distribution indicates that the periodic asymptotic state is confined within a bounded region depicted in Fig. 4(c) in red color.

To confirm the transition of the system from a chaotic state to a periodic state, we utilize the finite-time Lyapunov exponent (FTLE), which quantifies the amount of stretching or folding experienced by a trajectory along a specific direction over a finite time interval. This is illustrated in Fig. 4(d), which shows the maximum Lyapunov exponent for each oscillator in the system. During the extended transient state, the system demonstrates chaotic behavior, as indicated by the positive values of the Lyapunov exponent. These positive values confirm the chaotic behavior in the transient state. Subsequently, as the system evolves, it transitions into a periodic state. This transition is validated by all the Lyapunov exponent becoming non-positive at $t \sim 1.43 \times 10^5$, signifying that the system has settled into a stable periodic behavior.

B. Transient lifetime

To validate the transient lifetime and the escape rate from the proposed network, a finite-time Lyapunov exponent analysis was performed to differentiate the transient and asymptotic behaviors of the system. Specifically, we considered finite-time largest Lyapunov exponent $\lambda_{\max} \leq 0$ to denote periodic behavior and other positive values of $\lambda_{\max}$ as indicating chaotic state. In the transient chaotic regime, the distribution of transient chaos is dependent on the initial conditions of the system. The system parameters are the same as the TEE values and the hub oscillator initial conditions $x_h(0)$ are varied in the range of 0–2.5 and we have plotted the phase diagram in the ($x_h(0)$-t) plane, as illustrated in Fig. 5. For these initial conditions, the finite-time Lyapunov exponents were calculated using a total of 5×10^5 iterations. In Fig. 5, the regions exhibiting chaotic behavior are shown in the gray color region, while regions showing periodic behaviors are denoted by the red color region. The lifetime of transient chaos is measured as the duration from the initial time to the point when the largest Lyapunov exponent becomes negative. This process is repeated for a range of initial conditions of the central hub between 0 and 2.5. The mean value of these measurements is determined to be $t \sim 146\,351$, representing the average transient lifetime.

C. Generalized extreme value (GEV) distribution

To study the probability distribution of the network across the coupling (ε), we calculated the generalized extreme value (GEV)

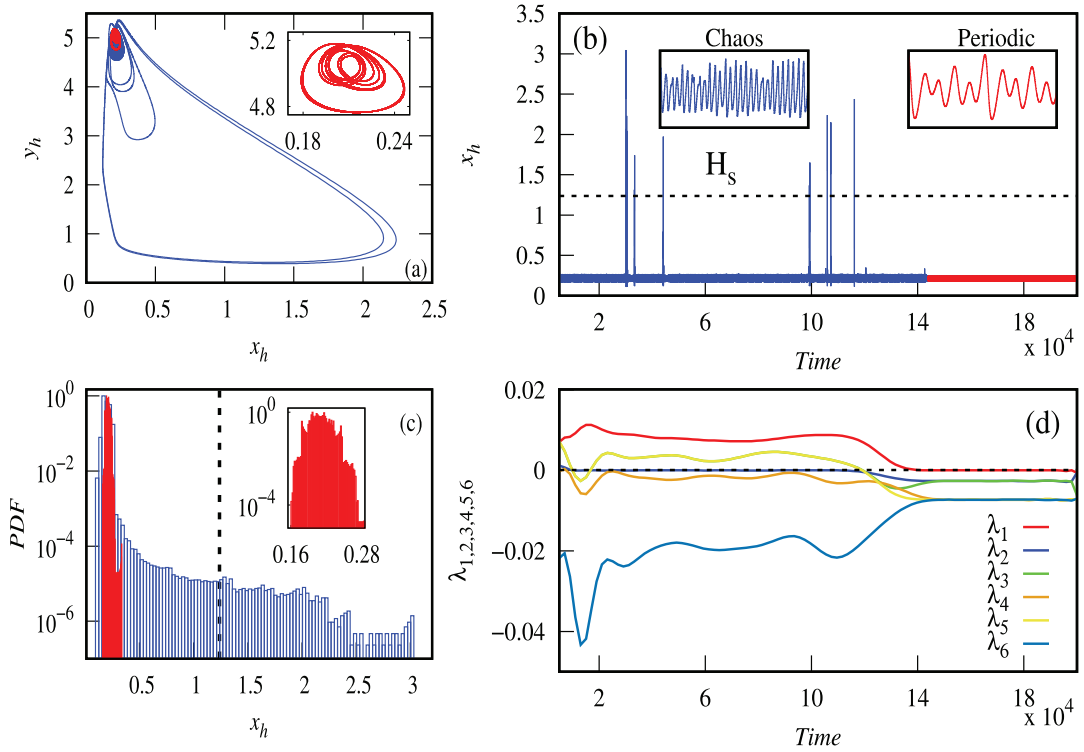

FIG. 4. Panel shows (a) the phase portrait in the $(x_h - y_h)$ plane, with the asymptotic periodic state depicted in the subplot. (b) The time evolution of the central hub variable $x_h(t)$, with transient states shown in blue color with a subplot labeled "chaos" and asymptotic behavior in red color with a subplot labeled "periodic." The TEEs threshold H_s is indicated by a dashed black line. (c) The probability distribution function (PDF), with the asymptotic periodic distribution depicted in the subplot and (d) the corresponding finite-time Lyapunov exponent (FTLE) of the time series $(x_h(t))$ for $\varepsilon = 0.6$.

distribution,[40] a primary statistical model in extreme value theory.[41] GEV allowed us to determine the shape of the tail, where extreme events occur. GEV distribution is widely used across different disciplines, such as engineering, climatology, finance, and insurance.[42,43] This distribution offers a comprehensive framework to characterize these events, which is crucial for understanding extreme phenomena. From the bifurcation diagram in Fig. 2, we deduced that the network exhibits periodic behavior at weak and strong coupling (ε), as well as periodic intermittency. Consequently, these periodic states follow a discrete distribution. Therefore, we excluded these regions and performed calculations only for the states that fit the generalized extreme value distribution.

The cumulative distribution function of the generalized extreme value (GEV) distribution is calculated by

$$F(x;\mu,\rho,\xi) = \exp\left\{-\left[1+\xi\left(\frac{x-\mu}{\rho}\right)\right]^{-1/\xi}\right\},$$

where μ is the location parameter, ρ is the scale parameter, and ξ is the shape parameter. The shape of the distribution depends on the value of ξ. When ξ is negative, extreme events follow a Weibull distribution, and the tail of the distribution is bounded. Conversely, for positive ξ values, extreme events exhibit a Fréchet distribution, displaying a heavy-tailed distribution. In cases where ξ equals zero, the extreme value distribution mirrors a Gumbel distribution, showcasing an exponential decay in the tail of the distribution.

By examining the evolution of the sign of ξ with coupling strength (ε), as shown in Fig. 6, in this present study, we observe that the network (1) follows a Fréchet distribution $(\xi > 0)$, indicating a heavy-tailed distribution. This implies that the probability of observing extremely large values decays slowly, meaning that large deviations from the mean are possible and occur with a non-negligible probability. Although in many instances, a high shape parameter (ξ) induces the distribution to be more skewed to the right (indicating high amplitudes), this does not surpass the threshold due to frequent large amplitudes, as depicted in Fig. 6 by blue dots and in the subplot representing the PDF of non-extreme events for $\varepsilon = 0.2$. At certain coupling strengths, events that qualify with a minimum positive shape parameter (ξ) induce extreme events by exceeding the threshold value, depicted in Fig. 6 by red dots and in the subplot representing the PDF of extreme events for $\varepsilon = 0.4$.

The return period (or recurrence interval) for a generalized extreme value (GEV) distribution is the average interval of time between occurrences of an events,[44] which is calculated by

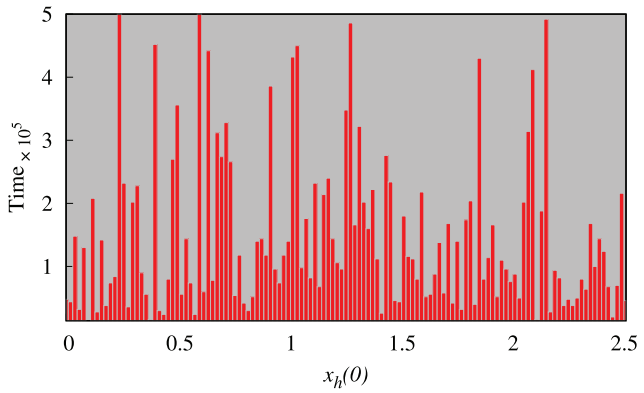

FIG. 5. The phase diagram constructed with initial conditions $x_h(0)$ vs transient time, using the finite-time Lyapunov exponent. In the periodic regime (gray color), the Lyapunov exponents have negative values. In the chaotic region (red color), the Lyapunov exponents have positive values.

$RP = \frac{1}{1-p_{(x_{peak})}}$, where $p_{(x_{peak})}$ is the empirical cumulative distribution function that represents the probability that a value is less than or equal to x_{peak}. In Fig. 7, the return period is plotted for the TEE parameters of the central hub oscillator with threshold (H_s) as the dashed horizontal line. From Fig. 7, it is evident that extreme events exceeding the threshold H_s have a long return period ranging from 200 to 6250, with the very low probability ($1/RP$) of occurrence of events between 0.005 and 1.6×10^{-4}. This indicates the rarity and infrequency of such occurrences, confirming the presence of extreme events in the network.

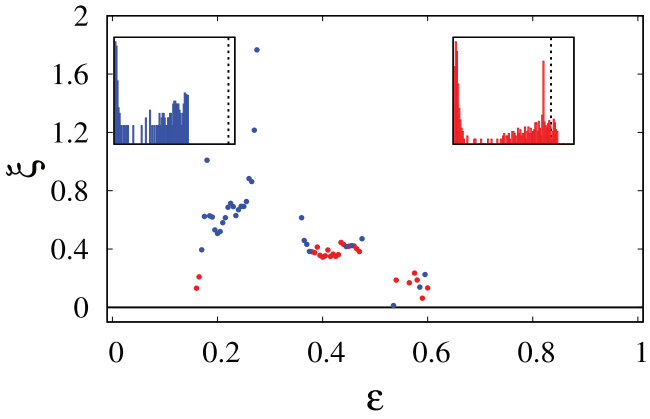

FIG. 6. The generalized extreme value distribution shape parameter ξ as a function of coupling strength ε is illustrated. Non-extreme events are shown in the blue color, while extreme events are depicted in the red color. The corresponding probability distribution function (PDF) is displayed in the subplots.

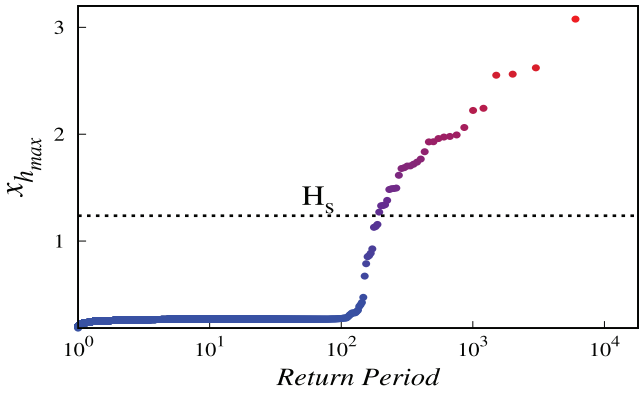

FIG. 7. The return period plot based on the generalized extreme value (GEV) distribution is shown, with the threshold marked by a vertical dashed line.

D. Average synchronization error

To study the synchronization of the network, the average synchronization error between the hub and the peripheral nodes of the network is measured, $\langle E \rangle \in [0, 1]$ defined by

$$\langle E \rangle = \frac{1}{T(N-1)} \sum_{j>1}^{N} \int_{t}^{t+T} ||x_j - x_1||\, dt',$$

where vector norm $||x|| = \sqrt{x^2 + y^2}$, a value of the average synchronization error ($\langle E \rangle$) equal to zero indicates no synchronization error, implying perfect or complete synchronization (CS) among the oscillators. Conversely, positive values of $\langle E \rangle$ indicate that the central oscillator is out of synchronization with the rest of the network oscillators.

Additionally, focus on the scenario where the peripheral nodes synchronize into a single cluster while the hub remains separate, forming its own distinct cluster. This phenomenon, known as remote synchronization (RS),[16] occurs when two or more nodes synchronize not through direct connections but via intermediate nodes. We introduce an additional measure to account for this situation. The average synchronization error for among peripheral $\langle E_p \rangle$ is measured by

$$\langle E_p \rangle = \frac{1}{T(N-1)} \sum_{j>2}^{N} \int_{t}^{t+T} ||x_j - x_2||\, dt'.$$

Hence, for our system, the average synchronization error $\langle E \rangle$ is calculated for both the transient and asymptotic states, which are shown in blue and red colors, respectively, as depicted in Fig. 8. The coherence among the peripheral nodes $\langle E_p \rangle$ is depicted in the green color. Figure 8 illustrates the average synchronization error ($\langle E \rangle$) across different coupling strengths (ε). These measurements have been computed from the numerical integration of system (1) using the parameter configuration for TEEs described in Sec. III A. From Fig. 8(a), it is clear that there is no notable difference in synchronization error between both the transient and asymptotic states of the network. The average synchronization error among the

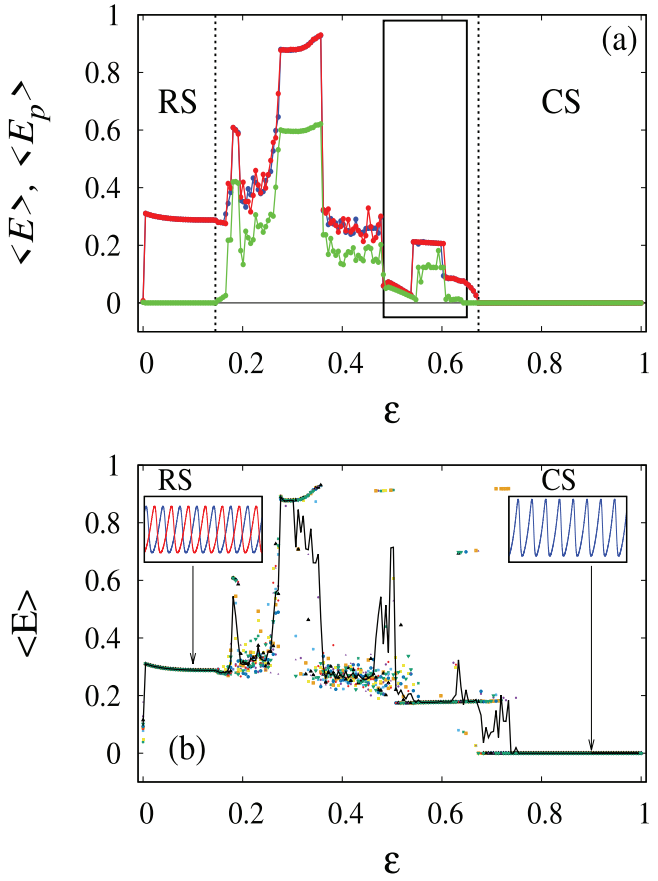

FIG. 8. Panel shows (a) the average synchronization error $\langle E \rangle$ for transient state depicted in the blue color and asymptotic state depicted in the red color. The average synchronization error of peripheral nodes $\langle E_p \rangle$, shown in the green color. The black rectangular box indicates the regime of transient extreme events (TEEs). (b) The average synchronization error $\langle E \rangle$ for a random set of initial conditions with subplots for remote synchronization (RS), complete synchronization (CS).

peripheral nodes suggests that the peripheral nodes are synchronized independently from the hub at weak coupling of $\varepsilon \in [0, 0.145]$, a phenomenon denoted as remote synchronization (RS).

At strong coupling of $\varepsilon \in [0.6733, 1]$, the network achieves complete synchronization (CS), as confirmed by the zero average synchronization error between the hub and peripherals depicted in blue color. In addition to understanding the synchronization dependence on initial conditions, we calculated the average synchronization error $\langle E \rangle$ for ten random sets of initial conditions, as shown in Fig. 8(b). The dark black color line indicates the calculated average of $\langle E \rangle$. It is evident that for any chosen initial conditions, the system exhibits remote synchronization at weak coupling and complete synchronization at strong coupling, as illustrated by the corresponding time series are shown as subplots in Fig. 8(b), with the hub depicted in the blue color and the peripheral nodes in the red color.

E. Energy function calculation

A mathematical framework to derive an energy function for chaotic systems, drawing upon the Hamiltonian formalism, is proposed by Sarasola *et al.*[45] In this formalism, the Hamiltonian function serves as an energy function for conservative systems, encapsulating the system's dynamics through its variables in phase space. For dissipative chaotic systems, where energy dissipation occurs, the dynamics are expressed as a sum comprising a skew-symmetric Poisson bracket and a symmetric bracket, termed the generalized Hamiltonian formalism. In general theory, in a dissipative dynamical system, energy is not conserved over time. This means that the total amount of energy in the system decreases due to dissipation or energy transfer. Therefore, in this section, the energy of our proposed network is calculated with respect to coupling coefficient and to explore how the energy transfers to one system to another system as well as the cumulative energy flows of the network. The velocity vector field $f(x)$ of an dissipative autonomous dynamical system can be separated into two distinct components,

$$f(x) = f_c(x) + f_d(x),$$

where f_c is a divergence-free vector field responsible for the complete rotational tensor and f_d is a gradient vector field carrying the entirety of whole divergence. The change in the system's energy along a trajectory is solely attributable to the contribution from f_d; the energy is dissipated, passively or actively, due to the divergent component of the velocity vector field, Thus, it obeys the relation

$$\nabla H^T f_d(x) = \dot{H}. \tag{2}$$

For each dynamical system, there exists a partial differential equation from which the energy function $H(x)$ can be determined by

$$\nabla H^T f_c(x) = 0. \tag{3}$$

A solution H which is satisfied by Eq. (3) of the system equation (1) represented by the non-definite quadratic form,

$$H = y_1 - \frac{bx_1^2}{2a} + \sum_{m=2}^{N} \frac{y_m}{N-1} - \frac{bx_m^2}{2a(N-1)},$$

in accordance with Eq. (2), the rate of change of Hamilton energy along a trajectory of the system (1) is

$$\dot{H} = \frac{bx_1^3 y_1 - bx_1^2 - b^2 x_1^2}{a} + x_1^2 y_1 + \sum_{m=2}^{N} \frac{bx_m^3 y_m - bx_m^2 - b^2 x_m^2}{a(N+1)} + \frac{x_m^2 y_m}{(N+1)}.$$

These energy calculations are very useful for examining the changes in average Hamilton energy within a network. We evaluated the total mean Hamilton energy for a range of coupling strengths ε, from 0 to 1, while keeping other system parameters constant as used for TEEs. The calculated results are shown in Fig. 9, where the cumulative energy of all oscillators is represented by the green line. The red and blue lines represent in subsets showing how the energy of the central hub and one peripheral node change, respectively.

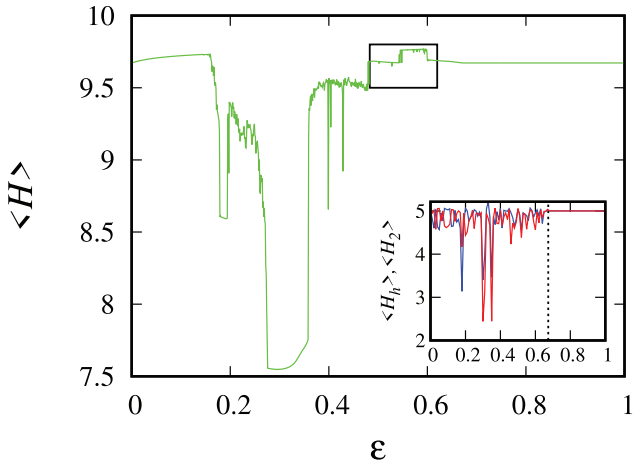

FIG. 9. The cumulative average Hamiltonian energy $\langle H \rangle$ of the network as a function of coupling strength ε. Here, the subplot indicates the average Hamiltonian energy of the central hub and peripheral node ($n = 2$) depicted in red and blue colors, respectively.

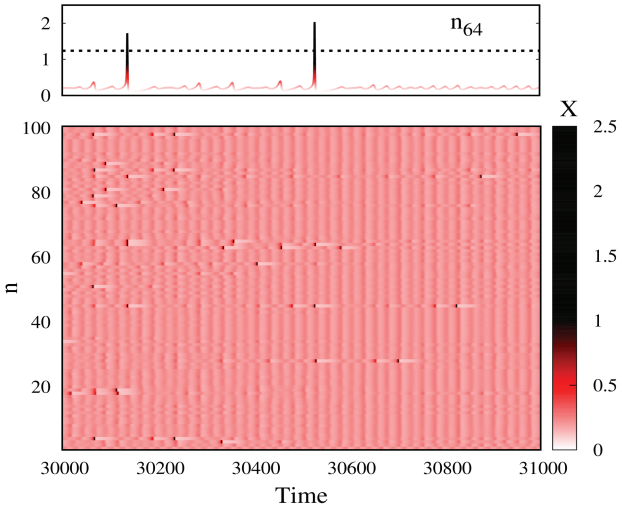

FIG. 10. The top panel displays the temporal plot of x_h for node index $n = 64$ in a network of $N = 100$ oscillators, with the threshold indicated by a horizontal line, while the bottom panel depicts the spatiotemporal pattern of a network with $N = 100$ oscillators. The dark black gradient color indicates the large amplitude of EEs in the network.

In Fig. 9, we can see that when the coupling strength (ε) is low, the cumulative energy (H) remains constant and evolves linearly due to remote synchronization. However, there is a sudden change in energy when the coupling strength ranges from $\varepsilon \in (0.19, 0.62)$ and the system transitions into a chaotic state. These abrupt changes in the transition of cumulative energy indicate that there is an exchange of energy between the hub and its peripherals. The network exhibits chaotic oscillations. During this range of coupling strength (ε), the system displays a variety of complex dynamics such as extreme events, generalized synchronization, transient chaos, and more. Furthermore, under strong coupling ($\varepsilon \in (0.62, 1.0)$), the total energy remains stable, and the individual oscillator energies of the hub and peripherals are synchronized. This is illustrated in the subplot of Fig. 9 and indicates perfect or complete synchronization (CS) in the system.

By analyzing the energy diagram, we observed that at the coupling parameter value $\varepsilon = 0.67$ (marked by the vertical dotted line), the system undergoes a transition from a desynchronized chaotic state to a synchronized periodic state. During this transition period, the system exhibits typical transient chaos before establishing a strong coupling that leads to a synchronized periodic regime. This transient chaos exhibits extreme events within it and is characterized as transient extreme events (TEEs). Further to check the robustness of extreme events (EEs) and transient extreme events (TEEs) in networks of different sizes, we plotted the spatiotemporal pattern of a network with $N = 100$ oscillators, which exhibits extreme events in all oscillators. This is depicted in Fig. 10, where the black gradient color indicates the large amplitude of extreme events (EEs) in the network, as qualified by the threshold from the respective temporal data. Additionally, the top panel of Fig. 10 shows the temporal plot for a peripheral node, chosen as node index $n = 64$ as an example, with the threshold line indicated. Additionally, we plotted the two-parameter diagram in the parameter space of (ε, N) for ε ranging from 0 to 1 and network sizes chosen in the range of $N = 3$–15 oscillators, as shown in Fig. 11. This diagram distinguishes the periodic and chaotic states using the largest Lyapunov exponent, with periodic states depicted in gray color and chaotic states (non-extreme events) in green color and extreme events were classified based on a threshold value H_s. Additionally, to differentiate between transient extreme events (TEEs) and typical extreme events (EEs), we performed calculations for both the transient and asymptotic states, with TEEs shown in blue color and EEs in red color. From Fig. 11, similar results are observed as depicted in Figs. 2 and 8, the system exhibits a periodic state in both weak and strong coupling regimes and displays transient extreme events (TEEs) before achieving complete synchronization.

IV. POSSIBLE APPLICATION

We have discussed some possible applications based on our results. In particular, our results on TEEs support some perspectives of applications for researchers and policymakers in various fields of domain. For instance, the integration of renewable energy sources into the power grid can also introduce transient power fluctuations, which may manifest as extreme events and transient.[29] Understanding and predicting these TEEs can be crucial for developing strategies to mitigate their impact, thereby improving the overall reliability and robustness of power grids.

Understanding the mechanisms behind long transients and their implications for forecasting is now a key challenge in both theoretical and empirical ecology. The identification of mechanisms that drive these transients, along with an understanding of the scaling laws governing their lifetimes could significantly enhance

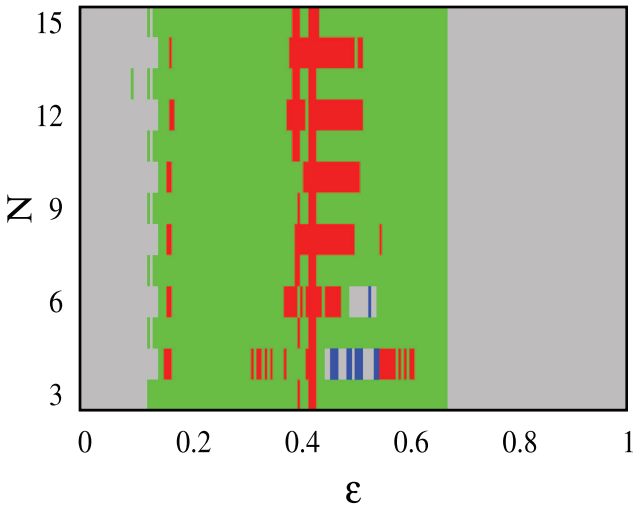

FIG. 11. The two-parameter diagram in the parameter space of (ε, N) illustrates the dynamical behavior of the network across a range of oscillators, from $N = 3$ to 15. Blue points represent the parameter values where TEEs exist, red points indicate the existence of EEs, green color points denote non-extreme events (chaotic states), and gray color points signify periodic states.

the accuracy of long-term forecasting and improve crisis anticipation. The study of transient extreme events (TEEs) offers a valuable perspective for addressing these challenges. By examining the mechanisms underlying long transients within ecosystems,[46] researchers can develop a unifying theory that integrates both physical and ecological insights. The application of TEEs in ecological contexts holds the potential to bridge gaps in current research and paves the way for advancements in the quantitative analysis of ecological transients.

On the other hand, the network of Brusselator provides a valuable framework for studying pattern formation, particularly through the analysis of sudden expansions (extreme events) and transient extreme events (TEEs). These phenomena offer insights into how oscillatory behavior within the network can lead to the emergence of spatial patterns, such as stripes or spots. Beyond chemical reactions, the Brusselator model has been extended to study pattern formation in other systems, including neural networks and ecological systems, where similar mechanisms of diffusion and instability play crucial roles. The application of the theoretical Brusselator star coupled network to transient extreme events could involve studying how these networks respond to sudden changes or perturbations, resulting in extreme behaviors. This approach could provide valuable insights into the mechanisms driving extreme events across various systems.

V. CONCLUSION

In this study, we observed the transition of a network from a chaotic (unsynchronized) state to a periodic (synchronized) state as the coupling strength was varied. During this transition, extreme events (EEs) emerged in a chemical model configured in a star network. Our analysis reveals that the proposed model exhibits complex dynamics, including the occurrence of extreme events. Specifically, we identified prolonged excursions of trajectories away from the bounded attractor during the transient state, with chaotic attractors displaying rare higher-amplitude events characterized as transient extreme events (TEEs). To confirm the presence of extreme events (EEs) and transient extreme events (TEEs), we determined a critical threshold through statistical methods. The dynamical transitions of the attractors and the occurrence of transient extreme events were analyzed using finite-time Lyapunov exponents. The observed extreme events were further validated through statistical analyses, including the probability distribution function, generalized extreme value distribution, and return period plots, to ensure the rarity of these events, and the transition to synchronization was confirmed by measuring the average synchronization error. Additionally, we calculated energy variations to verify the sudden expansions and transitions within the network. This research sheds light on the conditions under which extreme events can arise during prolonged transient states, significantly enhancing our understanding of such events in physical, engineering, and natural systems exhibiting transient dynamics.

ACKNOWLEDGMENTS

K.T. acknowledges the Chennai Institute of Technology for the experimental and computational assistance. S.S. acknowledges the Basic Research Program of the National Research University, Higher School of Economics, Moscow.

AUTHOR DECLARATIONS

Conflict of Interest

The authors have no conflicts to disclose.

Author Contributions

S. V. Manivelan: Conceptualization (equal); Data curation (equal); Formal analysis (equal); Investigation (equal); Methodology (equal); Resources (equal); Software (equal); Validation (equal); Visualization (equal); Writing – original draft (equal). **S. Sabarathinam:** Conceptualization (equal); Data curation (equal); Formal analysis (equal); Investigation (equal); Methodology (equal); Software (equal); Supervision (equal); Validation (equal); Visualization (equal); Writing – original draft (equal). **K. Thamilmaran:** Conceptualization (equal); Formal analysis (equal); Investigation (equal); Methodology (equal); Resources (equal); Supervision (equal); Writing – original draft (equal); Writing – review & editing (equal). **I. Manimehan:** Conceptualization (equal); Data curation (equal); Formal analysis (equal); Funding acquisition (equal); Investigation (equal); Methodology (equal); Project administration (equal); Resources (equal); Supervision (equal); Visualization (equal); Writing – original draft (equal); Writing – review & editing (equal).

DATA AVAILABILITY

The data that support the findings of this study are available from the corresponding author upon reasonable request.

REFERENCES

[1]S. L. Kingston, K. Thamilmaran, P. Pal, U. Feudel, and S. K. Dana, "Extreme events in the forced Liénard system," Phys. Rev. E **96**, 052204 (2017).
[2]S. Kumarasamy and A. N. Pisarchik, "Extreme events in systems with discontinuous boundaries," Phys. Rev. E **98**, 032203 (2018).
[3]P. Moitra and S. Sinha, "Emergence of extreme events in networks of parametrically coupled chaotic populations," Chaos **29**, 023131 (2019).
[4]G. Ansmann, R. Karnatak, K. Lehnertz, and U. Feudel, "Extreme events in excitable systems and mechanisms of their generation," Phys. Rev. E **88**, 052911 (2013).
[5]E. Zio and T. Aven, "Industrial disasters: Extreme events, extremely rare. Some reflections on the treatment of uncertainties in the assessment of the associated risks," Process Saf. Environ. Prot. **91**, 31–45 (2013).
[6]H. Kunreuther and E. Michel-Kerjan, "Dealing with extreme events: New challenges for terrorism risk coverage in the US," Center for Risk Management and Decision Processes, Wharton School, University of Pennsylvania (2004).
[7]A. Ray, A. Mishra, D. Ghosh, T. Kapitaniak, S. K. Dana, and C. Hens, "Extreme events in a network of heterogeneous Josephson junctions," Phys. Rev. E **101**, 032209 (2020).
[8]V. Kishore, M. Santhanam, and R. Amritkar, "Extreme events on complex networks," Phys. Rev. Lett. **106**, 188701 (2011).
[9]G. Gandhi and M. Santhanam, "Biased random walkers and extreme events on the edges of complex networks," Phys. Rev. E **105**, 014315 (2022).
[10]V. Kishore, A. R. Sonawane, and M. Santhanam, "Manipulation of extreme events on scale-free networks," Phys. Rev. E **88**, 014801 (2013).
[11]Y.-Z. Chen, Z.-G. Huang, H.-F. Zhang, D. Eisenberg, T. P. Seager, and Y.-C. Lai, "Extreme events in multilayer, interdependent complex networks and control," Sci. Rep. **5**, 17277 (2015).
[12]S. N. Chowdhury, S. Majhi, M. Ozer, D. Ghosh, and M. Perc, "Synchronization to extreme events in moving agents," New J. Phys. **21**, 073048 (2019).
[13]M. Baiesi and M. Paczuski, "Scale-free networks of earthquakes and aftershocks," Phys. Rev. E **69**, 066106 (2004).
[14]R. Albert and A.-L. Barabási, "Statistical mechanics of complex networks," Rev. Mod. Phys. **74**, 47 (2002).
[15]C. Meena, K. Murali, and S. Sinha, "Chimera states in star networks," Int. J. Bifurc. Chaos **26**, 1630023 (2016).
[16]A. Bergner, M. Frasca, G. Sciuto, A. Buscarino, E. J. Ngamga, L. Fortuna, and J. Kurths, "Remote synchronization in star networks," Phys. Rev. E **85**, 026208 (2012).
[17]J. Gómez-Gardenes, S. Gómez, A. Arenas, and Y. Moreno, "Explosive synchronization transitions in scale-free networks," Phys. Rev. Lett. **106**, 128701 (2011).
[18]N. Schwartz and L. Stone, "Exact epidemic analysis for the star topology," Phys. Rev. E **87**, 042815 (2013).
[19]M. P. Van den Heuvel and O. Sporns, "Network hubs in the human brain," Trends Cognit. Sci. **17**, 683–696 (2013).
[20]M. A. Bertolero, B. T. Yeo, D. S. Bassett, and M. D'Esposito, "A mechanistic model of connector hubs, modularity and cognition," Nat. Human Behav. **2**, 765–777 (2018).
[21]A. Khaledi-Nasab, J. A. Kromer, L. Schimansky-Geier, and A. B. Neiman, "Variability of collective dynamics in random tree networks of strongly coupled stochastic excitable elements," Phys. Rev. E **98**, 052303 (2018).
[22]P. Durairaj, S. Kanagaraj, S. Kumarasamy, and K. Rajagopal, "Emergence of extreme events in a quasiperiodic oscillator," Phys. Rev. E **107**, L022201 (2023).
[23]G. Ahlers and R. Walden, "Turbulence near onset of convection," Phys. Rev. Lett. **44**, 445 (1980).
[24]P. Turchin and S. P. Ellner, "Living on the edge of chaos: Population dynamics of Fennoscandian voles," Ecology **81**, 3099–3116 (2000).
[25]A. Yousefpour, H. Jahanshahi, J. M. Munoz-Pacheco, S. Bekiros, and Z. Wei, "A fractional-order hyper-chaotic economic system with transient chaos," Chaos, Solitons Fractals **130**, 109400 (2020).
[26]L. Zhu, A. Raghu, and Y.-C. Lai, "Experimental observation of superpersistent chaotic transients," Phys. Rev. Lett. **86**, 4017 (2001).
[27]M. Aron, T. Lilienkamp, S. Luther, and U. Parlitz, "Predicting the duration of chaotic transients in excitable media," J. Phys.: Complex. **2**, 035016 (2021).
[28]X.-S. Yang and Q. Yuan, "Chaos and transient chaos in simple Hopfield neural networks," Neurocomputing **69**, 232–241 (2005).
[29]L. Halekotte, A. Vanselow, and U. Feudel, "Transient chaos enforces uncertainty in the British power grid," J. Phys.: Complex. **2**, 035015 (2021).
[30]S. N. Chowdhury, A. Ray, S. K. Dana, and D. Ghosh, "Extreme events in dynamical systems and random walkers: A review," Phys. Rep. **966**, 1–52 (2022).
[31]A. Zumdieck, M. Timme, T. Geisel, and F. Wolf, "Long chaotic transients in complex networks," Phys. Rev. Lett. **93**, 244103 (2004).
[32]R. Zillmer, N. Brunel, and D. Hansel, "Very long transients, irregular firing, and chaotic dynamics in networks of randomly connected inhibitory integrate-and-fire neurons," Phys. Rev. E **79**, 031909 (2009).
[33]D. Dudkowski, P. Jaros, and T. Kapitaniak, "Extreme transient dynamics," Chaos **32**, 121101 (2022).
[34]R. Schmitz, K. Graziani, and J. L. Hudson, "Experimental evidence of chaotic states in the Belousov–Zhabotinskii reaction," J. Chem. Phys. **67**, 3040–3044 (1977).
[35]I. R. Epstein, "Coupled chemical oscillators and emergent system properties," Chem. Commun. **50**, 10758–10767 (2014).
[36]A. F. Taylor, M. R. Tinsley, and K. Showalter, "Insights into collective cell behaviour from populations of coupled chemical oscillators," Phys. Chem. Chem. Phys. **17**, 20047–20055 (2015).
[37]M. M. Norton, N. Tompkins, B. Blanc, M. C. Cambria, J. Held, and S. Fraden, "Dynamics of reaction-diffusion oscillators in star and other networks with cyclic symmetries exhibiting multiple clusters," Phys. Rev. Lett. **123**, 148301 (2019).
[38]S. Manivelan, S. Sabarathinam, K. Thamilmaran, and I. Manimehan, "Dynamical instabilities cause extreme events in a theoretical Brusselator model," Chaos, Solitons Fractals **180**, 114582 (2024).
[39]D. Dudkowski, J. Wojewoda, K. Czołczyński, and T. Kapitaniak, "Is it really chaos? The complexity of transient dynamics of double pendula," Nonlinear Dyn. **102**, 759–770 (2020).
[40]V. Lucarini, D. Faranda, J. M. M. de Freitas, M. Holland, T. Kuna, M. Nicol, M. Todd, S. Vaienti *et al.*, *Extremes and Recurrence in Dynamical Systems* (John Wiley & Sons, 2016).
[41]M. Ghil, P. Yiou, S. Hallegatte, B. Malamud, P. Naveau, A. Soloviev, P. Friederichs, V. Keilis-Borok, D. Kondrashov, V. Kossobokov, O. Mestre, C. Nicolis, H. W. Rust, P. Shebalin, M. Vrac, A. Witt, and I. Zaliapin, "Extreme events: Dynamics, statistics and prediction," Nonlinear Process. Geophys. **18**, 295–350 (2011).
[42]E. Castillo, *Extreme Value Theory in Engineering* (Elsevier, 2012).
[43]L. Haan and A. Ferreira, *Extreme Value Theory: An Introduction* (Springer, 2006), Vol. 3.
[44]E. J. Gumbel, "The return period of flood flows," Ann. Math. Stat. **12**, 163–190 (1941).
[45]C. Sarasola, F. Torrealdea, A. d'Anjou, A. Moujahid, and M. Graña, "Energy balance in feedback synchronization of chaotic systems," Phys. Rev. E **69**, 011606 (2004).
[46]A. Morozov, K. Abbott, K. Cuddington, T. Francis, G. Gellner, A. Hastings, Y.-C. Lai, S. Petrovskii, K. Scranton, and M. L. Zeeman, "Long transients in ecology: Theory and applications," Phys. Life Rev. **32**, 1–40 (2020).